

1 **Contrasting responses of phytoplankton productivity between coastal and offshore**
2 **surface waters in the Taiwan Strait and the South China Sea to short-term seawater**
3 **acidification**

4

5 Guang Gao¹, Tifeng Wang¹, Jiazhen Sun¹, Xin Zhao¹, Lifang Wang¹, Xianghui Guo¹,
6 Kunshan Gao^{1,2*}

7 ¹State Key Laboratory of Marine Environmental Science & College of Ocean and Earth
8 Sciences, Xiamen University, Xiamen 361005, China

9 ²Co-Innovation Center of Jiangsu Marine Bio-industry Technology, Jiangsu Ocean
10 University, Lianyungang 222005, China

11

12 *Corresponding author: ksgao@xmu.edu.cn

13

14 **Abstract**

15 Seawater acidification (SA) has been documented to either inhibit or enhance or result in
16 no effect on marine primary productivity (PP). In order to examine effects of SA in
17 changing environments, we investigated the influences of SA (a decrease of 0.4 pH_{total}
18 units with corresponding CO_2 concentrations ranged 22.0–39.7 μM) on PP through
19 deck-incubation experiments at 101 stations in the Taiwan Strait and the South China Sea-
20 (SCS), including the continental shelf and slope, as well as deep-water basin. The daily
21 primary productivities in surface seawater under incident solar radiation ranged from 17–
22 306 $\mu\text{g C} (\mu\text{g Chl } a)^{-1} \text{d}^{-1}$, with the responses of PP to SA being region-dependent and the
23 SA-induced changes varying from -88% (inhibition) to 57% (enhancement). The
24 SA-treatment stimulated PP in surface waters of coastal, estuarine and shelf waters, but
25 suppressed it in the South China Sea basin. Such SA-induced changes in PP were
26 significantly related to in situ pH and solar radiation in surface seawater, but negatively
27 related to salinity changes. Our results indicate that phytoplankton cells are more
28 vulnerable to a pH drop in oligotrophic waters. Contrasting responses of phytoplankton
29 productivity in different areas suggest that SA impacts on marine primary productivity
30 are region-dependent and regulated by local environments.

31 **Keywords:** CO_2 ; Taiwan Strait; seawater acidification; photosynthesis; primary
32 productivity; South China Sea

33 **1 Introduction**

34 The oceans have absorbed about one-third of anthropogenically released CO₂, which
35 increased dissolved CO₂ and decreased pH of seawater (Gattuso et al., 2015), leading to
36 ocean acidification (OA). This process is ongoing and likely intensifying (IPCC, 2019).
37 OA has been shown to result in profound influences on marine ecosystems (see the
38 reviews and literature therein, Mostofa et al., 2016; Doney et al., 2020). Marine
39 photosynthetic organisms, which contribute about half of the global primary production,
40 are also being affected by OA (see the reviews and literatures therein, Riebesell et al.,
41 2018; Gao et al., 2019a). In addition to the slow change of ocean acidification, some
42 processes, such as freshwater inputs, upwelling, typhoon and eddies, can lead to
43 instantaneous CO₂ rising ~~and short-term changes in carbonate chemistry, termed and~~
44 seawater acidification (SA) (Moreau et al., 2017; Yu et al., 2020). Since ~~seawater-~~
45 ~~acidification~~SA occurs in many locations of ocean, it is important to understand the
46 responses of the key players of marine biological CO₂ pump, the phytoplankton, to
47 seawater acidification.

48 Elevated CO₂ is well recognized to lessen the dependence of algae and
49 cyanobacteria on energy-consuming CO₂ concentrating mechanisms (CCMs) which
50 concentrate CO₂ around Rubisco, the key site for photosynthetic carbon fixation (Raven
51 & Beardall, 2014 and references therein; Hennon et al., 2015). The energy freed up from
52 the down-regulated CCMs under increased CO₂ concentrations can be applied to other
53 metabolic processes, resulting in a modest increase in algal growth (Wu et al., 2010;

54 Hopkinson et al., 2011; Xu et al., 2017). Accordingly, elevated CO₂ availability could
55 potentially enhance marine primary productivity (Schippers et al., 2004). For instance,
56 across 18 stations in the central Atlantic Ocean primary productivity was stimulated by
57 15–19% under elevated dissolved CO₂ concentrations up to 36 μM (Hein and
58 Sand-Jensen 1997). On the other hand, neutral effects of seawater acidification (SA) on
59 growth rates of phytoplankton communities were reported in five of six CO₂
60 manipulation experiments in the coastal Pacific (Tortell et al., 2000). Furthermore,
61 simulated future SA reduced surface PP in pelagic surface waters of Northern [SCS-South](#)
62 [China Sea](#) and East China Sea (Gao et al., 2012). It seems that the impacts of SA on PP
63 could be region-dependent. The varying effects of SA may be related to the regulation of
64 other factors such as light intensity (Gao et al., 2012), temperature (Holding et al., 2015),
65 nutrients (Tremblay et al., 2006) and community structure (Dutkiewicz et al., 2015).

66 Taiwan Strait of the East China Sea, located between southeast Mainland China and
67 the Taiwan Island, is an important channel in transporting water and biogenic elements
68 between the East China Sea (~~ECS~~) and the South China Sea (~~SCS~~). Among the Chinese
69 coastal areas, the Taiwan Strait is distinguished by its unique location. In addition to
70 riverine inputs, it also receives nutrients from upwelling (Hong et al., 2011). Primary
71 productivity is much higher in coastal waters than that in basin zones due to increased
72 supply of nutrients through river runoff and upwelling (Chen, 2003; Cloern et al., 2014).
73 The South China Sea (~~SCS~~), located from the equator to 23.8°N, from 99.1 to 121.1°E

74 and encompassing an area of about $3.5 \times 10^6 \text{ km}^2$, is one of the largest marginal seas in
75 the world. As a marginal sea of the Western Pacific Ocean, it has a deep semi-closed
76 basin (with depths $> 5000 \text{ m}$) and wide continental shelves, characterized by a tropical
77 and subtropical climate (Jin et al., 2016). Approximately 80% of ocean organic carbon is
78 buried in the Earth's continental shelves and therefore continental margins play an
79 essential role in the ocean carbon cycle (Hedges & Keil, 1995). Investigating how ~~ocean~~
80 acidificationSA affects primary productivity in the Taiwan Strait and the SCS-South
81 China Sea could help us to understand the contribution of marginal seas to carbon sink
82 under the future CO₂-increased scenarios. Although small-scale studies on SA impacts
83 have been conducted in the ESC-East China Sea and the South China SeaSCS (Gao et al.,
84 2012, 2017), our understanding of how SA affects PP in marginal seas is still fragmentary
85 and superficial. In this study, we conducted three cruises in the Taiwan Strait and the
86 South China SeaSCS, covering an area of $8.3 \times 10^5 \text{ km}^2$, and aimed to provide in-depth
87 insight into how SA and/or episodic pCO₂ rise affects PP in marginal seas with
88 comparisons to other types of waters.

89 **2 Materials and Methods**

90 **2.1 Investigation areas**

91 To study the impacts of projected SA (dropping by $\sim 0.4 \text{ pH}$) by the end of this
92 century (RCP8.5) on marine primary productivity in different areas (Gattuso et al., 2015),
93 we carried out deck-based experiments during the 3 cruises supported by National

94 Natural Science Foundation of China (NSFC), which took place in the Taiwan Strait (Jul
95 14th–25th, 2016), the South China Sea basin (Sep 6–24th, 2016), and the West South China
96 Sea (Sep 14th to Oct 24th, 2017), respectively. The experiments were conducted at 101
97 stations with coverage of 12 °N–26 °N and 110 °E–120 °E (Fig. 1). Investigation areas
98 include the continental shelf (0–200 m, 22 stations) and the slope (200–3400 m, 44
99 stations), and the vast deep-water basin (> 3400 m, 35 stations). In the continental shelf,
100 the areas with depth < 50 m are defined as coastal zones (9 stations).

101 **2.2 Measurements of temperature and carbonate chemistry parameters**

102 The temperature and salinity of surface seawater at each station were monitored with
103 an onboard CTD (Seabird, USA). pH_{NBS} was measured with an Orion 2-Star pH meter
104 (Thermo scientific, USA) that was calibrated with standard National Bureau of Standards
105 (NBS) buffers ($\text{pH}=4.01, 7.00, \text{ and } 10.01$ at $25.0\text{ }^{\circ}\text{C}$; Thermo Fisher Scientific Inc., USA).
106 After the calibration, the electrode of pH meter was kept in surface seawater for half an
107 hour and then the formal measurements were conducted. The analytical precision was
108 ± 0.001 . Total alkalinity (TA) was determined using Gran titration on a 25-mL sample
109 with a TA analyzer (AS-ALK1, Apollo SciTech, USA) that was regularly calibrated with
110 certified reference materials supplied by A. G. Dickson at the Scripps Institution of
111 Oceanography (Gao et al., 2018a). The analytical precision was $\pm 2\text{ }\mu\text{mol kg}^{-1}$. CO_2
112 concentration in seawater and the pH_{Total} (pH_{T}) values was calculated by using CO2SYS
113 (Pierrot et al., 2006) with the input of pH_{NBS} and TA data.

114 **2.3 Solar radiation**

115 The incident solar radiation intensity during the cruises was recorded with an
116 Eldonet broadband filter radiometer (Eldonet XP, Real Time Computer, Germany). This
117 device has three channels for PAR (400–700 nm), UV-A (315–400 nm) and UV-B (280–
118 315 nm) irradiance, respectively, which records the means of solar radiations over each
119 minute. The instrument was fixed at the top layer of the ship to avoid shading.

120 **2.4 Determination of primary productivity**

121 Surface seawater (0–1m) was collected a 10 L acid-cleaned (1 M HCl) plastic bucket
122 and pre-filtered (200 µm mesh size) to remove large grazers. To prepare high CO₂ (HC)
123 seawater, CO₂-saturated seawater was added into pre-filtered seawater until a decrease of
124 ~0.4 units in pH (corresponding CO₂ concentrations being 22.0–39.7 µM) was
125 approached (Gattuso et al., 2010). Seawater that was collected from the same location as
126 PP and filtered by cellulose acetate membrane (0.22 µm) was used to make the
127 CO₂-saturated seawater, which was made by directly flushing with pure CO₂ until pH
128 reached [values](#) around 4.50. When saturated-CO₂ seawater was added to the HC
129 treatment, equivalent filtered seawater (without flushing with CO₂) was also added to the
130 [ambient CO₂ \(AC\)](#) treatment as a control. The ratios of added saturated-CO₂ seawater to
131 incubation seawater were about 1:1000. ~~Seawater Samples was were~~ incubated within
132 half an hour after they were collected. Prepared AC and HC seawater was allocated into
133 50-mL quartz tubes in triplicate, inoculated with 5 µCi (0.185 MBq) NaH¹⁴CO₃ (ICN

134 Radiochemicals, USA), and then incubated for 24 h (over a day-night cycle) under 100 %
135 incident solar irradiances in a water bath for temperature control by running through
136 surface seawater. Due to heating by the deck, the temperatures in the water bath were 0–2
137 °C higher than in situ surface seawater temperatures. TA and pH of seawater before and
138 after 24h incubation were measured to monitor the changes of carbonate systems. After
139 the incubation, the cells were filtered onto GF/F filters (Whatman) and immediately
140 frozen at –20 °C for later analysis. In the laboratory, the frozen filters were transferred to
141 20 mL scintillation vials, thawed and exposed to HCl fumes for 12 h, and dried (55 °C, 6
142 h) to expel non-fixed ¹⁴C, as previously reported (Gao et al., 2017). Then 3 mL
143 scintillation cocktail (Perkin Elmer®, OptiPhase HiSafe) was added to each vial. After 2
144 h of reaction, the incorporated radioactivity was counted by a liquid scintillation counting
145 (LS 6500, Beckman Coulter, USA). The carbon fixation for 24 h incubation was taken as
146 chlorophyll (Chl) *a*-normalized daily primary productivity (PP, μg C (μg Chl *a*)⁻¹) (Gao et
147 | al., 2017). The changes (%) of PP induced by [ocean acidification SA](#) were expressed as
148 $(PP_{HC} - PP_{AC}) / PP_{AC} \times 100$, where PP_{HC} and PP_{AC} are the daily primary productivity under
149 HC and AC, respectively.

150 **2.5 Chl *a* measurement**

151 Pre-filtered (200 μm mesh size) surface seawater (500–2000 mL) at each station was
152 filtered onto GF/F filter (25 mm, Whatman) and then stored at -80 °C. After returning to
153 laboratory, phytoplankton cells on the GF/F filter were extracted overnight in absolute

154 methanol at 4 °C in darkness. After centrifugation (5000 g for 10 min), the absorption
155 values of the supernatants were analyzed by a UV–VIS spectrophotometer (DU800,
156 Beckman, Fullerton, California, USA). The concentration of chlorophyll *a* (Chl *a*) was
157 calculated according to Porra (2002).

158 **2.6 Data analysis**

159 The data of environmental parameters were expressed in raw and the data of PP were
160 the means of triplicate incubations. Two-way analysis of variance (ANOVA) was used to
161 analyze the effects of SA and location on PP. Least significant difference (LSD) was used
162 to for *post hoc* analysis. Linear fitting analysis was conducted with Pearson correlation
163 analysis to assess the relationship between PP and environmental factors. A 95%
164 confidence level was used in all analyses.

165 **3 Results**

166 During the cruises, surface temperature ranged from 25.0 to 29.9 °C in the Taiwan
167 Strait and from 27.1 to 30.2 °C in the South China Sea (Fig. 2a). Surface salinity ranged
168 from 30.0 to 34.0 in the Taiwan Strait and from 31.0 to 34.3 in the South China Sea (Fig.
169 2b). The lower salinities were found in the estuaries of Minjiang and Jiulong Rivers as
170 well as Mekong River-induced Rip current. High salinities were found in the [South China](#)
171 [SeaSCS](#) basin. Surface pH_T changed between 7.99–8.20 in the Taiwan Strait with the
172 higher values in the estuary of Minjiang River (Fig. 2c). Compared to the Taiwan Strait,
173 the South China Sea had lower surface pH (7.91–8.08) with the lowest value near the

174 island in the Philippines. TA ranged from 2100 to 2359 $\mu\text{mol kg}^{-1}$ SW in the Taiwan
175 Strait and 2126 to 2369 $\mu\text{mol kg}^{-1}$ SW in the South China Sea (Fig. 2d). The lowest value
176 occurred in the estuary of Minjiang River. CO_2 concentration in surface seawater changed
177 from 6.4–13.3 $\mu\text{M-mol kg}^{-1}$ SW in the Taiwan Strait, and 9.3–14.3 $\mu\text{M-mol kg}^{-1}$ SW in
178 the [South China SeaSCS](#) (Fig. 2e). It showed an opposite pattern to surface pH, with the
179 lowest value in the estuary of Minjiang River in the Taiwan Strait and highest value in
180 near the islands in the Philippines in the South China Sea. During the PP investigation
181 period, the daytime mean PAR intensity ranged from 126.6 to 145.2 $\text{W m}^{-2} \text{s}^{-1}$ in the
182 Taiwan Strait and 37.3 to 150.0 $\text{W m}^{-2} \text{s}^{-1}$ in the [South China SeaSCS](#) (Fig. 2f).

183 The concentration of Chl *a* ranged from 0.11 to 12.13 $\mu\text{g L}^{-1}$ in the Taiwan Strait (Fig.
184 3). The highest concentration occurred in the estuary of the Minjiang River. The
185 concentration of Chl *a* in the [South China SeaSCS](#) ranged from 0.037 to 7.43 $\mu\text{g L}^{-1}$. The
186 highest concentration was found in the coastal areas of Guangdong province in China.
187 For both the Taiwan Strait and the [South China SeaSCS](#), there were high Chl *a*
188 concentrations ($> 1.0 \mu\text{g L}^{-1}$) in coastal areas, particularly in the estuaries of the Minjing
189 River, Jiulong River and Pearl River. On the contrary, Chl *a* concentrations in offshore
190 areas were lower than $0.2 \mu\text{g L}^{-1}$.

191 Surface primary productivity changed from 99 ~~to~~ $-302 \mu\text{g C} (\mu\text{g Chl } a)^{-1} \text{d}^{-1}$ in the
192 Taiwan Strait, and from 17 ~~to~~ $306 \mu\text{g C} (\mu\text{g Chl } a)^{-1} \text{d}^{-1}$ in the South China Sea (Fig. 4).
193 High surface primary productivity ($> 200 \mu\text{g C} (\mu\text{g Chl } a)^{-1} \text{d}^{-1}$) was found in the

194 estuaries of the Minjing River, Jiulong River, and Pearl River and areas near the East of
195 Vietnam. In basin zones, the surface primary productivity was usually lower than 100 μg
196 C ($\mu\text{g Chl } a$)⁻¹ d⁻¹.

197 A series of onboard CO₂-enrich experiments in the investigated regions were
198 conducted during three cruises. In ~~the high CO₂HC~~ treatments, pH_{total} ~~had a decreased of~~
199 ~~by~~ 0.34–0.43 units, while pCO₂ and CO₂ ~~had an increase of~~ increased by 676–982 μatm
200 and 17–25 μM kg⁻¹ SW, respectively (Table S1). Carbonate chemistry parameters
201 after 24 h of incubation were stable ($\Delta\text{pH} < 0.06$, $\Delta\text{TA} < 53 \mu\text{mol kg}^{-1}$ SW), indicating
202 the successful manipulation (Table S1). It was observed that instantaneous effects of
203 elevated pCO₂ on primary productivity of surface phytoplankton community in all
204 investigated regions ranged from -88% (inhibition) to 57% (promotion), revealing
205 significant regional differences among continental shelf, slope and deep-water basin
206 (ANOVA, $F_{(4002, 40498)} = 43.403747$, $p \leq 0.004027$, Fig. 5). Among 101 stations, 70
207 stations showed insignificant SA effects. SA increased PP at 6 stations and reduced PP at
208 25 stations. Positive effects of SA on surface primary productivity were observed in the
209 Taiwan Strait and the western South China SeaSCS (Fig. 5, red-yellow shading areas),
210 with the maximal enhancement of 57% in the station approaching the Mekong River
211 plume (LSD, $p < 0.001$). Reductions in PP induced by the elevated CO₂ were mainly
212 found in the central South China SeaSCS basin within the latitudes of 10 °N to 14 °N and
213 the longitudes of 114.5 °E to 118 °E (Fig. 5, blue-purple shading areas), with inhibition

214 rates ranging from 24% to 88% (Fig. 5, LSD, $p < 0.05$). These results showed a
215 region-related effect of SA on photosynthetic carbon fixation of surface phytoplankton
216 assemblages. Overall, the elevated $p\text{CO}_2$ had neutral or positive effects on primary
217 productivity in the continental shelf and slope regions, while having adverse effects in the
218 deep-water basin.

219 By analyzing the correlations between SA-induced PP changes and regional
220 environmental parameters (Table S2), we found that SA-induced changes in
221 phytoplankton primary productivity was significantly positively related with *in situ* pH (p
222 < 0.001 , $r = 0.379$), and PAR density ($p = 0.002$, $r = 0.311$) (Fig. 6). On the other hand,
223 the influence induced by SA was negatively related to salinity that ranged from 30.00 to
224 34.28 ($p < 0.001$, $r = -0.418$).

225 **4 Discussion**

226 In the present study, we found that the elevated $p\text{CO}_2$ and associated pH drop
227 increased or did not affect PP in the continental shelf and slope waters but reduced it in
228 basin waters. Our results suggested that the enhanced effects of the SA treatment on
229 photosynthetic carbon fixation depend on regions of different physicochemical conditions,
230 including pH, light intensity and salinity. In addition, coastal diatoms appear to benefit
231 more from SA than pelagic ones (Li et al., 2016). Therefore, community structure
232 differences might also be responsible for the differences of the short-term high
233 CO_2 -induced acidification between coastal and basin waters.

234 SA is deemed to have two kinds of effects at least (Xu et al., 2017; Shi et al., 2019).
235 The first one is the enrichment of CO₂, which is usually beneficial for photosynthetic
236 carbon fixation and growth of algae because insufficient ambient CO₂ limits algal
237 photosynthesis (Hein & Sand-Jensen, 1997; Bach & Taucher, 2019). The other effect is
238 the decreased pH which could be harmful because it disturbs the acid-base balance
239 between extracellular and intracellular environments. For instance, the decreased pH
240 projected for future SA was shown to reduce the growth of the diazotroph *Trichodesmium*
241 (Hong et al., 2017), decrease PSII activity by reducing the removal rate of PsbD (D2)
242 (Gao et al., 2018b) and increase mitochondrial and photo-respirations in diatoms and
243 phytoplankton assemblages (Yang and Gao 2012, Jin et al., 2015). In addition, SA could
244 reduce the Rubisco transcription of diatoms, which also contributed to the decreased
245 growth (Endo et al., 2015). Therefore, the net impact of SA depends on the balance
246 between its positive and negative effects, leading to enhanced, inhibited or neutral
247 influences, as reported in diatoms (Gao et al., 2012, Li et al., 2021) and phytoplankton
248 assemblages in the Arctic and subarctic shelf seas (Hoppe et al., 2018), the North Sea
249 (Eberlein et al., 2017) and the South China Sea (Wu and Gao 2010, Gao et al., 2012). The
250 balance of positive and negative effects of SA can be regulated by other factors, including
251 pH, light intensity, salinity, population structure, etc. (Gao et al., 2019a, b; Xie et al.,
252 2022).

253 In the present study, SA increased or did not affect PP in coastal waters but reduced it

254 in offshore waters, which is significantly related to pH, light intensity and salinity (Fig. 6).
255 The effect of SA changed from negative to positive with the increase of local pH. The
256 higher pH occurred in coastal zones which may be caused by higher biomass of
257 phytoplankton (Fig. 3). Higher pH caused by intensive photosynthesis of phytoplankton
258 is accompanied with decreased CO₂ levels. In this case, CO₂ is more ~~limited~~ limiting for
259 photosynthesis of phytoplankton compared to lower pH. Therefore, SA could stimulate
260 primary productivity via supplying more available CO₂ (Hurd et al., 2019). On the other
261 hand, lower pH occurred in deep-water basin. Lower pH represents higher CO₂
262 availability. CO₂ is not limited or less limited in this case. Therefore, more CO₂ brought
263 by SA may not benefit photosynthesis of phytoplankton. Instead, decreased pH
264 accompanied by SA may inhibit photosynthesis or growth of phytoplankton, which is
265 found in cyanobacteria (Hong et al., 2017). Furthermore, the negative effects of SA are
266 particularly significant when nutrient is limited (Li et al., 2018). The nutrient levels in the
267 basin are usually lower than on the shelf (Yuan et al., 2011; Lu et al., 2020; Du et al.,
268 2021), which may exacerbate the negative effects of ~~OA-SA~~ in the basin zone.

269 The negative effects of SA disappeared with ~~the increase of~~ ing light intensity in this
270 study. This results in inconsistent with Gao et al (2012)' study, in which SA increased
271 photosynthetic carbon fixation of three diatoms (*Phaeodactylum tricornutum*,
272 *Thalassiosira pseudonana* and *Skeletonema costatum*) under lower light intensities but
273 ~~increased~~ decreased it under higher light intensities. The divergent findings may be due to

274 different population structure that varies in different areas. Coastal zones where nutrients
275 are relatively sufficient usually have abundant diatoms while picophytoplanktons mainly
276 *Prochlorococcus* and *Synechococcus*, dominate oligotrophic areas (Xiao et al., 2018,
277 Zhong et al., 2020). In this study, most investigated areas are oligotrophic and thus the
278 response of local phytoplankton to the combination of light intensity and SA may be
279 different from diatoms. Meanwhile, the weak correlation ($r = 0.311$) between light
280 intensity and SA effect suggests the deviation from linear relationship in the context of
281 multiple variables needs to be further illuminated in future studies. It is worth noting that
282 the samples were not mixed down in the water bath in the present study and exposed
283 to the 100% incident solar irradiances ~~may have high light stress on cells~~. Lower incident
284 solar irradiances or some devices can be used to simulate seawater mixing in future
285 studies. A Negative-negative correlation between SA-induced changes of PP and salinity
286 was found in this study. The decrease of salinity (from 35 to 30) has been shown to
287 alleviate the negative effect of SA on photosynthetic carbon fixation of a
288 coccolithorporid *Emiliana huxleyi* (Xu et al., 2020) although the potential mechanisms
289 remain unknown. On the other hand, the change of salinity (from 6 to 3) did not affect
290 effective quantum yield of microplanktonic community in the Baltic Sea grown under
291 different CO₂ levels (Wulff et al., 2018). In this study, ~~we presume that~~ the negative
292 relationship between salinity and SA effects seems to be an autocorrelation between
293 salinity and in situ pH (Fig. S1) ~~may be mainly related to local pH~~ because lower salinity

294 | occurred in coastal waters where seawater pH was higher while the basin zone usually
295 | had higher salinities and lower pH.

296 | The specific environmental conditions have profound effects on shaping diverse
297 | dominant phytoplankton groups (Boyd et al., 2010). Larger eukaryotic groups (especially
298 | diatoms) usually dominate the complex coastal regions, while picophytoplanktons
299 | (*Prochlorococcus* and *Synechococcus*), characterizing with more efficient nutrients
300 | uptake, dominate the relatively stable offshore waters (Dutkiewicz et al., 2015). In
301 | summer and early autumn, previous investigations demonstrated that diatoms dominated
302 | in the northern waters and the Taiwan Strait (coastal and shelf regions) with ~~the~~ high
303 | abundances of phytoplankton, which ~~are~~ is consistent with our Chl *a* data;
304 | *Prochlorococcus* and *Synechococcus* dominated in the South China SeaSCS basin and the
305 | north of South China SeaSCS (slope and basin regions) (Xiao et al., 2018, Zhong et al.,
306 | 2020). In addition, it has been reported that larger cells benefit more from SA because a
307 | thicker diffusion layer around the cells limits the transport of CO₂ (Feng et al., 2010; Wu
308 | et al., 2014). In contrast, a thinner diffusion layer and higher surface to volume ratio in
309 | smaller phytoplankton cells can make them easier to transport CO₂ near the cell surface
310 | and within the cells, and therefore picophytoplankton species are less CO₂-limited (Bao
311 | and Gao, 2021). Therefore, different community structures between coastal and basin
312 | areas could also be responsible for the enhanced and inhibitory effects of SA. It is worth
313 | noting that seasonality may also lead to the differential effects of SA on primary

314 productivity since the Taiwan Strait cruise was conducted in July and the cruises of the
315 South China Sea basin and the West South China Sea were conducted in September. The
316 SST and solar PAR intensity of the Taiwan Strait in July was 2–3 °C and $22 \pm 22 \text{ W m}^{-2}$
317 s^{-1} higher than that in September (Zhang et al., 2008, 2009; Table S3). Although the
318 effects of SA were not related to temperature as shown in this study (Table S2), the higher
319 solar radiation in July may contribute to the positive effect of SA on primary productivity.
320 [In addition, species succession of phytoplankton with season may also affect the response](#)
321 [to SA \(Xiao et al., 2018\).](#)

322 **5 Conclusions**

323 By investigating the impacts of the elevated pCO_2 on PP in the Taiwan Strait and the
324 [South China SeaSCS](#), we demonstrated that such short SA-treatments induced changes in
325 PP were mainly related to pH, light intensity and salinity based on Pearson correlation
326 coefficients, supporting the hypothesis that negative impacts of SA on PP increase from
327 coastal to basin waters (Gao et al., 2019a). [In addition, phytoplankton community](#)
328 [structures may also modulate SA induced changes-](#). In view of ocean climate changes,
329 strengthened stratification due to global warming would reduce the upward transports of
330 nutrients and thus marine primary productivity. The negative effect of SA in basin zones
331 ~~would~~ [may](#) further reduce primary productivity. Meanwhile, PP in [some](#) coastal waters
332 ~~would~~ [may](#) be increased by SA. -

333 *Data availability.* All data are included in the article or Supplement.

334 *Author contributions.* KG and TW developed the original idea and designed research.

335 TW and JS carried out fieldwork. GG provided statistical analyses and prepared figures.

336 GG, KG, and XZ wrote the manuscript. All contributed to revising the paper.

337 *Competing interests.* The contact author has declared that neither they nor their

338 co-authors have any competing interests.

339 *Disclaimer.* Publisher's note: Copernicus Publications remains neutral with regard to

340 jurisdictional claims in published maps and institutional affiliations.

341 *Acknowledgements.* This work was supported by the National Natural Science

342 Foundation of China (41720104005, 41890803, 41721005, and 42076154) and the

343 Fundamental Research Funds for the Central Universities (20720200111). The authors

344 are grateful to the students He Li, Xiaowen Jiang and Shanying Tong, and the laboratory

345 technicians Xianglan Zeng and Wenyan Zhao. We appreciate the NFSC Shiptime Sharing

346 Project (project number: 41849901) for supporting the Taiwan Strait cruise

347 (NORC2016-04). We appreciate the chief scientists Yihua Cai, Huabin Mao and Chen Shi

348 and the R/V Yanping II, Shiyan I and Shiyan III for leading and conducting the cruises.

349 **References**

350 Bach, L. T., and Taucher, J.: CO₂ effects on diatoms: a synthesis of more than a decade of

351 ocean acidification experiments with natural communities, *Ocean Sci.*, 15,

352 1159-1175, 2019.

353 Bao, N., and Gao, K.: Interactive effects of elevated CO₂ concentration and light on the

354 picophytoplankton *Synechococcus*, *Front. Mar. Sci.*, 8, 1-7, 2021.

355 Boyd, P. W., Strzepek, R., Fu, F. X., and Hutchins, D. A.: Environmental control of open-
356 ocean phytoplankton groups: Now and in the future, *Limnol. Oceanogr*, 55,
357 1353-1376, 2010.

358 Chen, C. T. A.: Rare northward flow in the Taiwan Strait in winter: A note, *Cont. Shelf*
359 *Res.*, 23, 387-391, 2003.

360 Cloern, J. E., Foster, S.Q. and Kleckner, A. E.: Phytoplankton primary production in the
361 world's estuarine-coastal ecosystems, *Biogeosciences*, 11, 2477-2501, 2014.

362 Doney, S. C., Busch, D. S., Cooley, S. R., and Kroeker, K. J.: The impacts of ocean
363 acidification on marine ecosystems and reliant human communities, *Annu. Rev. Env.*
364 *Resour.*, 45, 83-112, 2020.

365 Du, C., He, R., Liu, Z., Huang, T., Wang, L., Yuan, Z., Xu, Y., Wang, Z. and Dai, M.:
366 Climatology of nutrient distributions in the South China Sea based on a large data
367 set derived from a new algorithm. *Prog. Oceanogr.*, 195, 102586, 2021.

368 Dutkiewicz, S., Morris, J. J., Follows, M. J., Scott, J., Levitan, O., Dyhrman, S. T., and
369 Berman-Frank, I.: Impact of ocean acidification on the structure of future
370 phytoplankton communities, *Nat. Clim. Change*, 5, 1002-1006, 2015.

371 Eberlein, T., Wohlrab, S., Rost, B., John, U., Bach, L. T., Riebesell, U., and Van de Waal,
372 D. B.: Effects of ocean acidification on primary production in a coastal North Sea
373 phytoplankton community, *Plos One*, 12, 1-15, 2017.

374 Endo, H., Sugie, K., Yoshimura, T., and Suzuki, K.: Effects of CO₂ and iron availability
375 on *rbcL* gene expression in Bering Sea diatoms, *Biogeosciences*, 12, 2247-2259,
376 2015.

377 Feng, Y., Hare, C. E., Rose, J. M., Handy, S. M., DiTullio, G. R., Lee, P. A., Smith, W. O.,
378 Peloquin, J., Tozzi, S., Sun, J., Zhang, Y., Dunbar, R. B., Long, M. C., Sohst, B.,
379 Lohan, M., and Hutchins, D. A.: Interactive effects of iron, irradiance and CO₂ on
380 Ross Sea phytoplankton, *Deep-Sea Res. PT. I*, 57, 368-383, 2010.

381 ~~Flynn, K. J., Blackford, J. C., Baird, M. E., Raven, J. A., Clark, D. R., Beardall, J.,~~
382 ~~Brownlee, C., Fabian, H., and Wheeler, G. L.: Changes in pH at the exterior surface~~
383 ~~of plankton with ocean acidification, *Nat. Clim. Change*, 2, 510-513, 2012.~~

384 Gao, G., Xu, Z. G., Shi, Q., and Wu, H. Y.: Increased CO₂ exacerbates the stress of
385 ultraviolet radiation on photosystem II function in the diatom *Thalassiosira*
386 *weissflogii*, *Environ. Exp. Bot.*, 156, 96-105, 2018b.

387 Gao, G., Jin, P., Liu, N., Li, F. T., Tong, S. Y., Hutchins, D. A., and Gao, K. S.: The
388 acclimation process of phytoplankton biomass, carbon fixation and respiration to the
389 combined effects of elevated temperature and *p*CO₂ in the northern South China Sea,
390 *Mar. Pollut. Bull.*, 118, 213-220, 2017.

391 Gao, G., Qu, L., Xu, T., Burgess, J.G., Li, X. and Xu, J.: Future CO₂-induced ocean
392 acidification enhances resilience of a green tide alga to low-salinity stress. *ICES J.*
393 *Mar. Sci.*, 76, 2437-2445, 2019b.

394 Gao, G., Xia, J. R., Yu, J. L., Fan, J. L., and Zeng, X. P.: Regulation of inorganic carbon
395 acquisition in a red tide alga (*Skeletonema costatum*): The importance of phosphorus
396 availability, *Biogeosciences*, 15, 4871-4882, 2018a.

397 Gao, K. S., Beardall, J., Häder, D. P., Hall-Spencer, J. M., Gao, G., and Hutchins, D. A.:
398 Effects of ocean acidification on marine photosynthetic organisms under the
399 concurrent influences of warming, UV radiation, and deoxygenation, *Front. Mar.*
400 *Sci.*, 6, 1-18, 2019a.

401 Gao, K. S., Xu, J. T., Gao, G., Li, Y. H., Hutchins, D. A., Huang, B. Q., Wang, L., Zheng,
402 Y., Jin, P., Cai, X. N., Hader, D. P., Li, W., Xu, K., Liu, N. N., and Riebesell, U.:
403 Rising CO₂ and increased light exposure synergistically reduce marine primary
404 productivity, *Nat. Clim. Change*, 2, 519-523, 2012.

405 Gattuso, J. P., Gao, K. S., Lee, K., Rost, B., and Schulz, K. G.: Approaches and tools to
406 manipulate the carbonate chemistry, pp 41-52. Guide to best practices for ocean
407 acidification research and data reporting, edited by: Riebesell, U., Fabry, V. J.,
408 Hansson, L., and Gattuso J.-P., Luxembourg: Publications Office of the European
409 Union, 2010.

410 Gattuso, J. P., Magnan, A., Billé R., Cheung, W. W. L., Howes, E. L., Joos, F., Allemand,
411 D., Bopp, L., Cooley, S. R., Eakin, C. M., Hoegh-Guldberg, O., Kelly, R. P., Portner,
412 H. O., Rogers, A. D., Baxter, J. M., Laffoley, D., Osborn, D., Rankovic, A., Rochette,
413 J., Sumaila, U. R., Treyer, S., and Turley, C.: Contrasting futures for ocean and

414 society from different anthropogenic CO₂ emissions scenarios, *Science*, 349,
415 aac4722, 2015.

416 ~~Geider, R. J., La Roche, J., Greene, R. M., and Olaizola, M.: Response of the~~
417 ~~photosynthetic apparatus of *Phaeodactylum tricorutum* (Bacillariophyceae) to~~
418 ~~nitrate, phosphate, or iron starvation, *J. Phycol.*, 29, 755-766, 1993.~~

419 ~~Häder, D. P., Williamson, C. E., Wängberg, S. A., Rautio, M., Rose, K. C., Gao, K. S.,~~
420 ~~Helbling, E. W., Sinha, R. P., and Worrest, R.: Effects of UV radiation on aquatic~~
421 ~~ecosystems and interactions with other environmental factors, *Photoch. Photobio.*~~
422 ~~*Sci.*, 14, 108-126, 2015.~~

423 Hedges, J. I., and Keil, R. G.: Sedimentary organic matter preservation: an assessment
424 and speculative synthesis, *Mar. Chem.*, 49, 81-115, 1995.

425 Hein, M., and Sand-Jensen, K.: CO₂ increases oceanic primary production, *Nature*, 388,
426 526-527, 1997.

427 Hennon, G. M. M., Ashworth, J., Groussman, R. D., Berthiaume, C., Morales, R. L.,
428 Baliga, N. S., Orellana, M. V., and Armbrust, E. V.: Diatom acclimation to elevated
429 CO₂ via cAMP signalling and coordinated gene expression, *Nat. Clim. Change*, 5,
430 761-765, 2015.

431 ~~Hofmann, G. E., Smith, J. E., Johnson, K. S., Send, U., Levin, L. A., Micheli, F., Paytan,~~
432 ~~A., Price, N. N., Peterson, B., Takeshita, Y., Matson, P. G., Crook, E. D., Kroeker, K.~~
433 ~~J., Gambi, M. C., Rivest, E. B., Frieder, C. A., Yu, P. C., and Martz, T. R.:~~

434 [High frequency dynamics of ocean pH: A multi-ecosystem comparison, Plos One, 6,](#)
435 [1-11, 2011.](#)

436 Holding, J. M., Duarte, C. M., Sanz-Martín, M., Mesa, E., Arrieta, J. M., Chierici, M.,
437 Hendriks, I. E., Garcia-Corral, L. S., Regaudie-de-Gioux, A., Delgado, A., Reigstad,
438 M., Wassmann, P., and Agustí, S.: Temperature dependence of CO₂-enhanced
439 primary production in the European Arctic Ocean, *Nat. Clim. Change*, 5, 1079-1082,
440 2015.

441 Hong, H. S., Chai, F., Zhang, C. Y., Huang, B. Q., Jiang, Y. W., and Hu, J. Y.: An
442 overview of physical and biogeochemical processes and ecosystem dynamics in the
443 Taiwan Strait, *Cont. Shelf Res.*, 31, S3-S12, 2011.

444 Hong, H. Z., Shen, R., Zhang, F. T., Wen, Z. Z., Chang, S. W., Lin, W. F., Kranz, S. A.,
445 Luo, Y. W., Kao, S. J., Morel, F. M. M. and Shi, D. L.: The complex effects of ocean
446 acidification on the prominent N₂-fixing cyanobacterium *Trichodesmium*. *Science*,
447 356, 527-530, 2017.

448 Hopkinson, B. M., Dupont, C. L., Allen, A. E., and Morel, F. M.: Efficiency of the
449 CO₂-concentrating mechanism of diatoms, *P. Natl. Acad. Sci. USA.*, 108, 3830-3837,
450 2011.

451 Hoppe, C. J. M., Wolf, K. K. E., Schuback, N., Tortell, P. D., and Rost, B.: Compensation
452 of ocean acidification effects in Arctic phytoplankton assemblages. *Nat. Clim.*
453 *Change*, 8, 529-533, 2018.

454 Hurd, C.L., Beardall, J., Comeau, S., Cornwall, C.E., Havenhand, J.N., Munday, P.L.,
455 Parker, L.M., Raven, J.A. and McGraw, C.M.: Ocean acidification as a multiple
456 driver: how interactions between changing seawater carbonate parameters affect
457 marine life. *Mar. Freshwater Res.*, 71, 263-274, 2019.

458 IPCC, 2019: IPCC Special Report on the Ocean and Cryosphere in a Changing Climate
459 [H.-O. Pörtner, D.C. Roberts, V. Masson-Delmotte, P. Zhai, M. Tignor, E.
460 Poloczanska, K. Mintenbeck, A. Alegría, M. Nicolai, A. Okem, J. Petzold, B. Rama,
461 N.M. Weyer (eds.)]. In press.

462 Jin, P., Gao, G., Liu, X., Li, F. T., Tong, S. Y., Ding, J. C., Zhong, Z. H., Liu, N. N., and
463 Gao, K. S.: Contrasting photophysiological characteristics of phytoplankton
464 assemblages in the Northern South China Sea, *Plos One*, 11, 1-16, 2016.

465 Jin, P., Wang, T. F., Liu, N. N., Dupont, S., Beardall, J., Boyd, P. W., Riebesell, U., and
466 Gao, K. S.: Ocean acidification increases the accumulation of toxic phenolic
467 compounds across trophic levels, *Nat. Commun.*, 6, 1-6, 2015.

468 ~~Johnson, M. D., and Carpenter, R. C.: Nitrogen enrichment offsets direct negative effects~~
469 ~~of ocean acidification on a reef building crustose coralline alga, *Biol. Letters*, 14,~~
470 ~~1-5, 2018.~~

471 Li, F. T., Wu, Y. P., Hutchins, D. A., Fu, F. X., and Gao, K. S.: Physiological responses of
472 coastal and oceanic diatoms to diurnal fluctuations in seawater carbonate chemistry
473 under two CO₂ concentrations, *Biogeosciences*, 13, 6247-6259, 2016.

474 Li, F. T., Beardall, J., and Gao, K. S.: Diatom performance in a future ocean: interactions
475 between nitrogen limitation, temperature, and CO₂-induced seawater acidification,
476 ICES J. Mar. Sci., 75, 1451-1464, 2018.

477 ~~Li, G., Gao, K. S., Yuan, D. X., Zheng, Y., and Yang, G. Y.: Relationship of~~
478 ~~photosynthetic carbon fixation with environmental changes in the Jiulong River~~
479 ~~estuary of the South China Sea, with special reference to the effects of solar UV~~
480 ~~radiation, Mar. Pollut. Bull., 62, 1852-1858, 2011.~~

481 Li, H. X., Xu, T. P., Ma, J., Li, F. T., and Xu, J. T.: Physiological responses of
482 *Skeletonema costatum* to the interactions of seawater acidification and the
483 combination of photoperiod and temperature, Biogeosciences, 18, 1439-1449, 2021.

484 ~~Li, W., Gao, K., and Beardall, J.: Nitrate limitation and ocean acidification interact with~~
485 ~~UV B to reduce photosynthetic performance in the diatom *Phaeodactylum*~~
486 ~~*tricornutum*, Biogeosciences, 12, 2383-2393, 2015.~~

487 Lu, Z., Gan, J., Dai, M., Zhao, X. and Hui, C. R.: Nutrient transport and dynamics in the
488 South China Sea: A modeling study. Prog. Oceanogr., 183, 102308, 2020.

489 ~~McNicholl, C., Koch, M. S., and Hofmann, L. C.: Photosynthesis and light-dependent~~
490 ~~proton pumps increase boundary layer pH in tropical macroalgae: A proposed~~
491 ~~mechanism to sustain calcification under ocean acidification, J. Exp. Mar. Biol.~~
492 ~~Ecol., 521, 1-12, 2019.~~

493 Moreau, S., Penna, A. D., Llorc, J., Patel, R., Langlais, C., Boyd, P. W., Matear, R. J.,

494 Phillips, H. E., Trull, T. W., Tilbrook, B. and Lenton, A.: Eddy-induced carbon
495 transport across the Antarctic Circumpolar Current. *Global Biogeochem. Cy.*, 31,
496 1368-1386, 2017

497 Mostofa, K.M., Liu, C.Q., Zhai, W., Minella, M., Vione, D., Gao, K., Minakata, D.,
498 Arakaki, T., Yoshioka, T., Hayakawa, K. and Konohira, E.: Reviews and Syntheses:
499 Ocean acidification and its potential impacts on marine ecosystems, *Biogeosciences*,
500 13, 1767-1786, 2016.

501 Pierrot, D., Wallace, D.W. R., and Lewis, E.: MS Excel program developed for CO₂
502 system calculations. ORNL/CDIAC-105a, Carbon Dioxide Information Analysis
503 Center, Oak Ridge National Laboratory, US Department of Energy, Oak Ridge,
504 Tennessee, USA., 2006.

505 Porra, R. J.: The chequered history of the development and use of simultaneous equations
506 for the accurate determination of chlorophylls a and b, *Photosynth. Res.*, 73,
507 149-156, 2002.

508 Raven, J. A., and Beardall, J.: CO₂ concentrating mechanisms and environmental change,
509 *Aquat. Bot.*, 118, 24-37, 2014.

510 Schippers, P., Lüring, M., and Scheffer, M.: Increase of atmospheric CO₂ promotes
511 phytoplankton productivity, *Ecol. Lett.*, 7, 446-451, 2004.

512 Shi, D. L., Hong, H. Z., Su, X., Liao, L. R., Chang, S. W., and Lin, W. F.: The
513 physiological response of marine diatoms to ocean acidification: Differential roles of

514 seawater $p\text{CO}_2$ and pH, *J. Phycol.*, 55, 521-533, 2019.

515 [Taylor, A. R., Brownlee, C., and Wheeler, G. L.: Proton channels in algae: Reasons to be](#)
516 [excited, *Trends Plant Sci.*, 17, 675-684, 2012.](#)

517 Tortell, P. D., Rau, G. H., and Morel, F. M. M.: Inorganic carbon acquisition in coastal
518 Pacific phytoplankton communities, *Limnol. Oceanogr.*, 45, 1485-1500, 2000.

519 Tremblay, J. E., Michel, C., Hobson, K. A., Gosselin, M., and Price, N. M.: Bloom
520 dynamics in early opening waters of the Arctic Ocean. *Limnol. Oceanogr.*, 51,
521 900-912, 2006.

522 Riebesell, U., Aberle-Malzahn, N., Achterberg, E. P., Algueró-Muñiz, M.,
523 Alvarez-Fernandez, S., Arístegui, J., Bach, L. T., Boersma, M., Boxhammer, T.,
524 Guan, W. C., Haunost, M., Horn, H. G., Loscher, C. R., Ludwig, A., Spisla, C.,
525 Sswat, M., Stange, P., and Taucher, J.: Toxic algal bloom induced by ocean
526 acidification disrupts the pelagic food web, *Nat. Clim. Change*, 8, 1082-1086, 2018.

527 Wu, Y., Gao, K., and Riebesell, U.: CO_2 -induced seawater acidification affects
528 physiological performance of the marine diatom *Phaeodactylum tricorutum*,
529 *Biogeosciences*, 7, 2915-2923, 2010.

530 Wu, Y., Campbell, D. A., Irwin, A. J., Suggett, D. J., and Finkel, Z. V.: Ocean
531 acidification enhances the growth rate of larger diatoms. *Limnol. Oceanogr.*, 59,
532 1027-1034, 2014.

533 Wulff, A., Karlberg, M., Olofsson, M., Torstensson, A., Riemann, L., Steinhoff, F. S.,

534 Mohlin, M., Ekstrand, N., and Chierici, M.: Ocean acidification and desalination:
535 Climate-driven change in a Baltic Sea summer microplanktonic community, *Mar.*
536 *Biol.*, 165, 1-15, 2018.

537 ~~Wu, Y. P., and Gao, K. S.: Combined effects of solar UV radiation and CO₂-induced~~
538 ~~seawater acidification on photosynthetic carbon fixation of phytoplankton~~
539 ~~assemblages in the South China Sea. *Chinese Sci. Bull.*, 55, 3680-3686, 2010.~~

540 Xiao, W. P., Wang, L., Laws, E., Xie, Y. Y., Chen, J. X., Liu, X., Chen, B. Z., and Huang,
541 B. Q.: Realized niches explain spatial gradients in seasonal abundance of
542 phytoplankton groups in the South China Sea, *Prog. Oceanogr.*, 162, 223-239, 2018.

543 Xie, S., Lin, F., Zhao, X. and Gao, G.: Enhanced lipid productivity coupled with carbon
544 and nitrogen removal of the diatom *Skeletonema costatum* cultured in the high CO₂
545 level. *Algal Res.* 61, 102589, 2022.

546 Xu, J. K., Sun, J. Z., Beardall, J., and Gao, K. S.: Lower salinity leads to improved
547 physiological performance in the coccolithophorid *Emiliana huxleyi*, which partly
548 ameliorates the effects of ocean acidification, *Front. Mar. Sci.*, 7, 1-18, 2020.

549 Xu, Z. G., Gao, G., Xu, J. T., and Wu, H. Y.: Physiological response of a golden tide alga
550 (*Sargassum muticum*) to the interaction of ocean acidification and phosphorus
551 enrichment, *Biogeosciences*, 14, 671-681, 2017.

552 Yang, G. Y., and Gao, K. S.: Physiological responses of the marine diatom *Thalassiosira*
553 *pseudonana* to increased pCO₂ and seawater acidity, *Mar. Environ. Res.*, 79,

554 142-151, 2012.

555 ~~[Yoshimura, T., Nishioka, J., Suzuki, K., Hattori, H., Kiyosawa, H. and Watanabe, Y. W.:](#)~~
556 ~~[Impacts of elevated CO₂ on organic carbon dynamics in nutrient depleted Okhotsk](#)~~
557 ~~[Sea surface waters. J. Exp. Mar. Biol. Ecol., 395, 191-198, 2010.](#)~~

558 Yu, P., Wang, Z. A., Churchill, J., Zheng, M., Pan, J., Bai, Y., and Liang, C.: Effects of
559 typhoons on surface seawater pCO₂ and air-sea CO₂ fluxes in the northern South
560 China Sea. J. Geophys. Res-Oceans, 125, p.e2020JC016258, 2020.

561 Yuan, X., He, L., Yin, K., Pan, G., and Harrison, P. J.: Bacterial distribution and nutrient
562 limitation in relation to different water masses in the coastal and northwestern South
563 China Sea in late summer. Cont. Shelf Res., 31, 1214-1223, 2011.

564 ~~[Zhang, C., Zhang, X., Zeng, Y., Pan, W., Lin J.: Retrieval and validation of sea surface](#)~~
565 ~~[temperature in the Taiwan Strait using MODIS data. Acta Oceanol. Sin., 30, 153-160,](#)~~
566 ~~[2008.](#)~~

567 ~~[Zhang, C., Ren, Y., Cai, Y., Zeng, Y., and Zhang, X.: Study on local monitoring model for](#)~~
568 ~~[SST in Taiwan strait based on MODIS data. J. Trop. Meteorol., 25, 73-81, 2009.](#)~~

569 Zhong, Y. P., Liu, X., Xiao, W. P., Laws, E. A., Chen, J. X., Wang, L., Liu, S. G., Zhang,
570 F., and Huang, B. Q.: Phytoplankton community patterns in the Taiwan Strait match
571 the characteristics of their realized niches, Prog. Oceanogr., 186, 1-15, 2020.

572 **Figure captions**

573 **Fig. 1** Sampling stations for the incubation experiments in the Taiwan Strait and the
574 South China Sea during three cruises. Taiwan Strait cruise was conducted in July 2016
575 (red dots), South China Sea Basin cruise were conducted in September 2016 (blue dots)
576 and Western South China Sea cruise was conducted in September 2017 (black dots).

577 **Fig. 2** Temperature ($^{\circ}\text{C}$, panel a), salinity (panel b), pH_{total} (panel c), total alkalinity (μmol
578 $\text{L}^{-1} \text{SW}$, panel d), and CO_2 ($\mu\text{mol kg}^{-1} \text{SW}$, panel e) in surface seawater and mean PAR
579 intensity ($\text{W m}^{-2} \text{s}^{-1}$, panel f) during the PP incubation experiments.

580 **Fig. 3** Chl *a* concentration ($\mu\text{g L}^{-1}$) in the Taiwan Strait and the South China Sea during
581 research cruises.

582 **Fig. 4** Surface primary productivity ($\mu\text{g C } (\mu\text{g Chl } a)^{-1} \text{d}^{-1}$) in the Taiwan Strait and the
583 South China Sea during research cruises.

584 **Fig. 5** Ocean Seawater acidification (pH decreases of 0.4 units) induced changes (%) of
585 surface primary productivity in the Taiwan Strait and the South China Sea. Red-yellow
586 shading represents a positive effect on PP and blue-purple shading represents a negative
587 effect.

带格式的：下标

Fig. 6 Ocean-Seawater acidification (pH decreases of 0.4 units) induced changes (%) on surface primary productivity (%) in the South China Sea as a function of ambient pH_{total} (a), PAR (b), and salinity (c). The dotted lines represent 95% confidence intervals.

带格式的: 下标

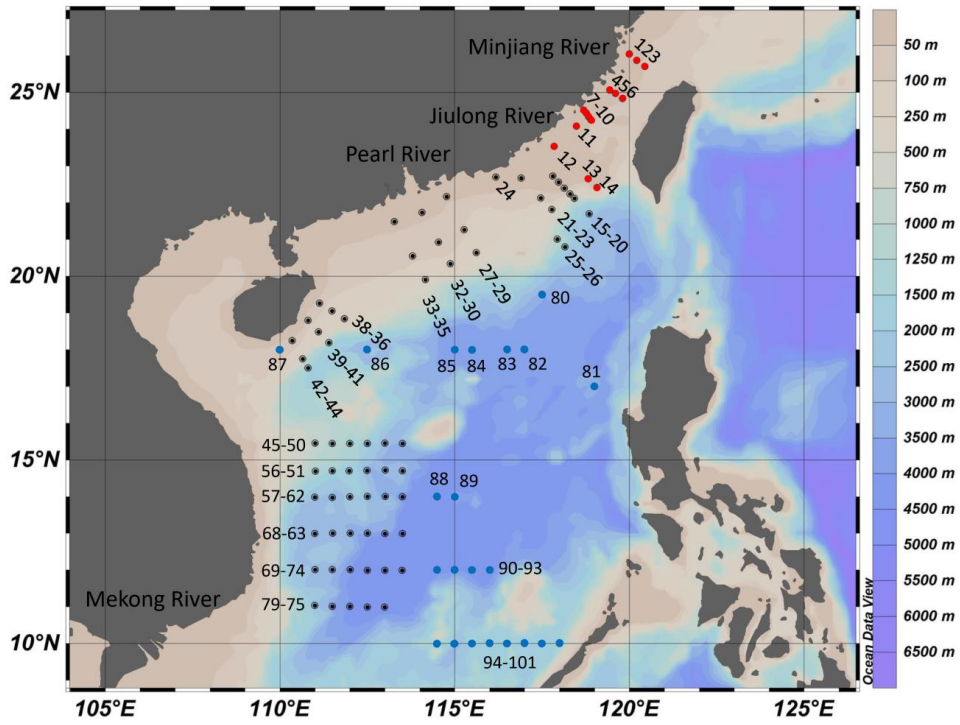
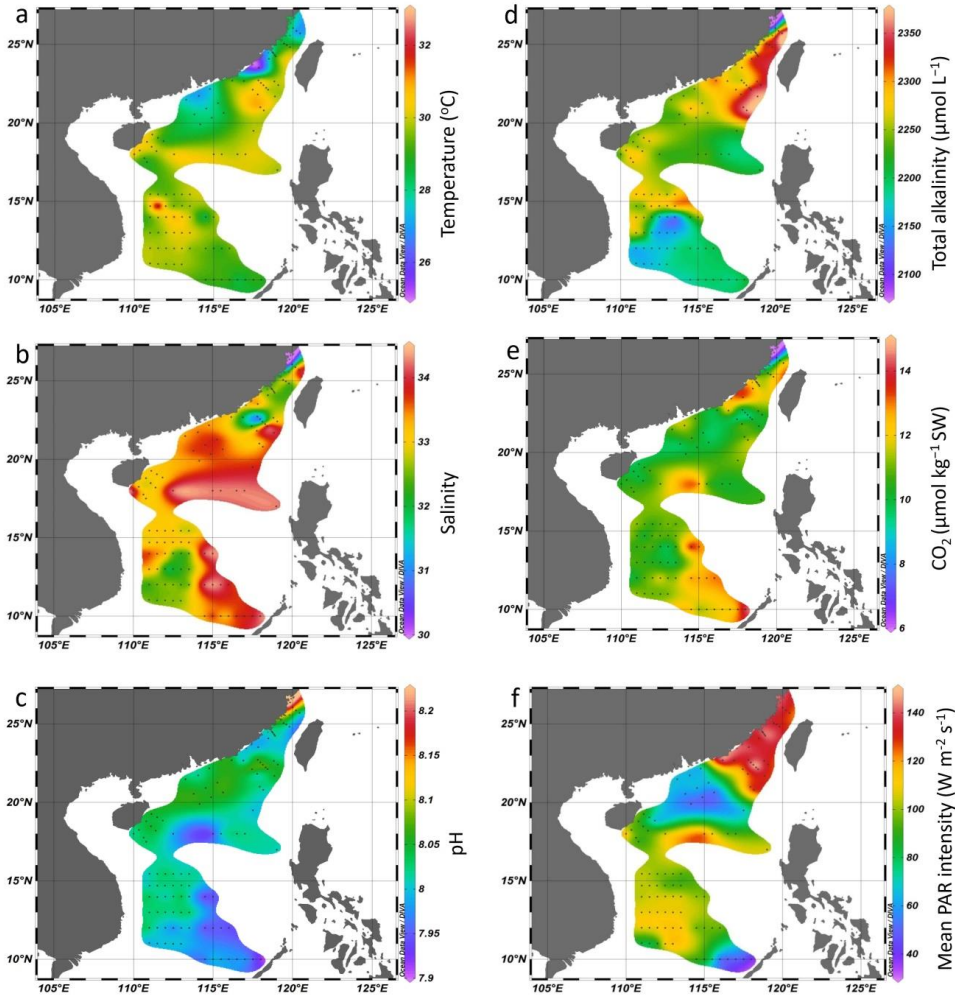


Fig. 1



带格式的: 字体: (默认) Times New Roman, 小四, 字体颜色: 文字 1

带格式的: 缩进: 左侧: 0 厘米, 悬挂缩进: 2 字符

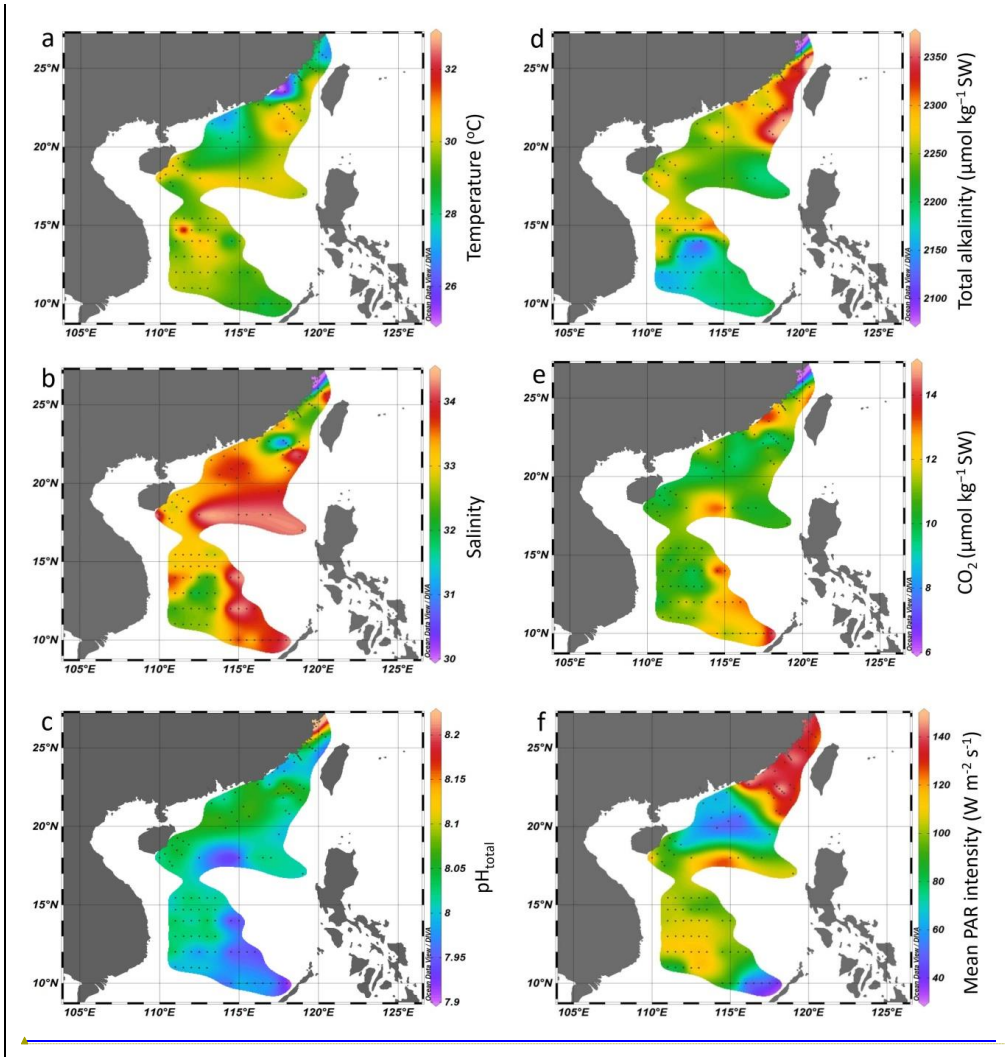


Fig. 2

带格式的: 字体: (默认) Times New Roman, 小四, 字体颜色: 文字 1

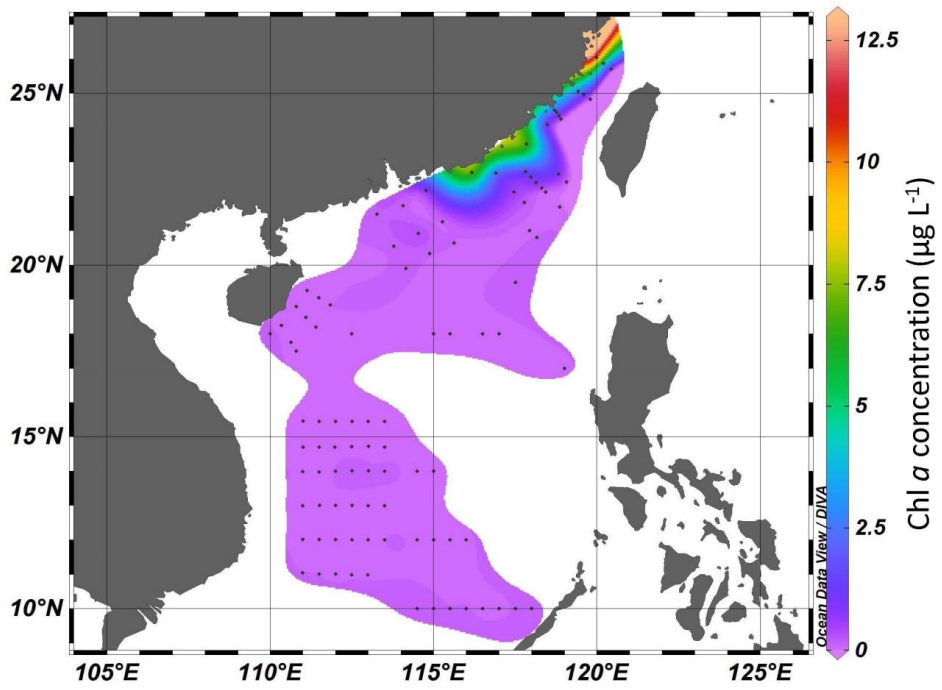


Fig. 3

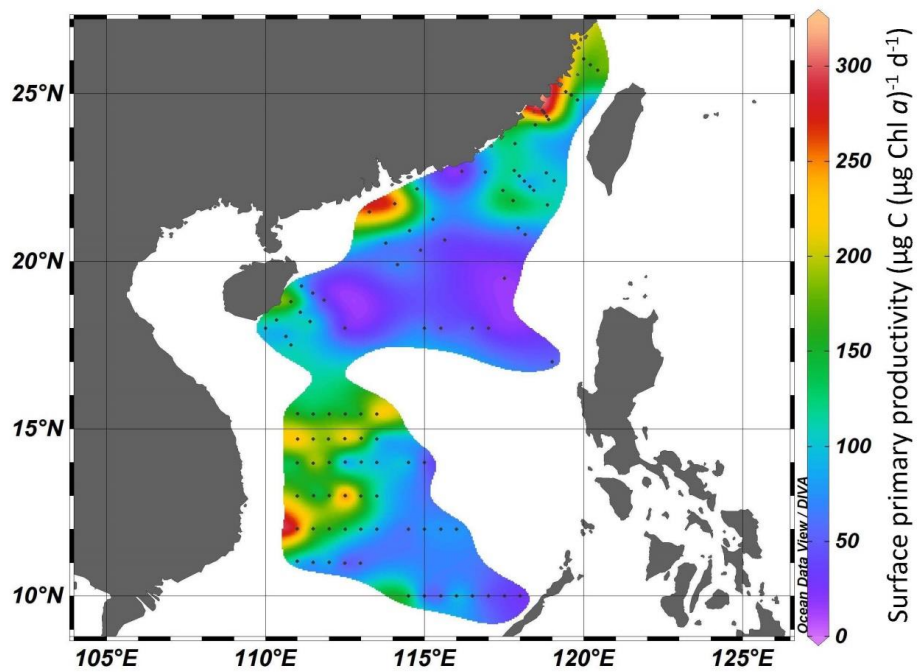
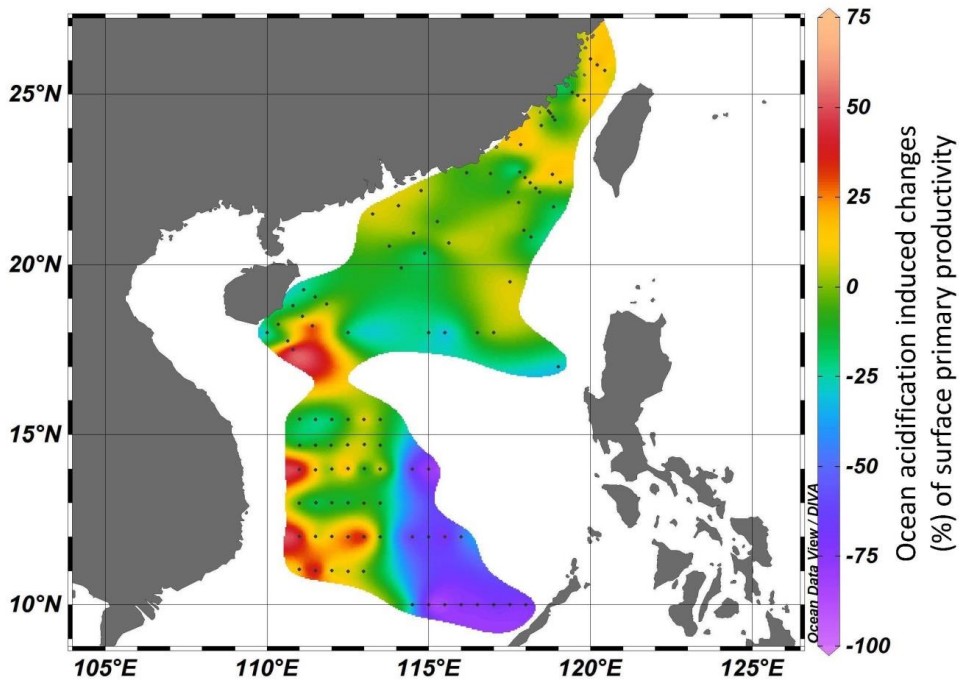
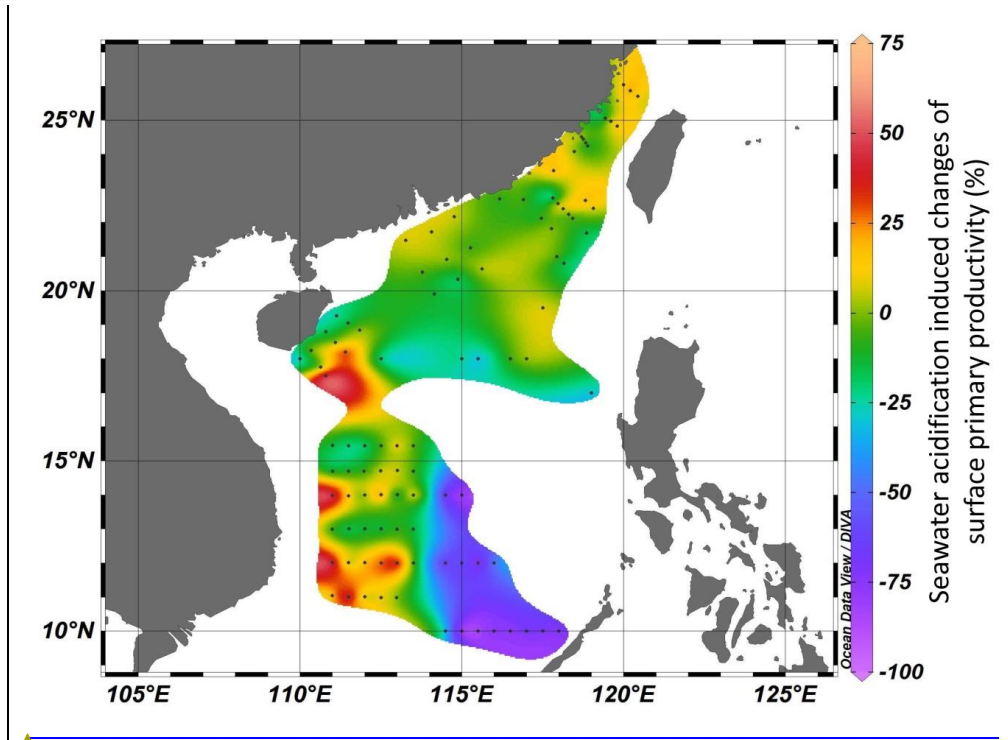


Fig. 4



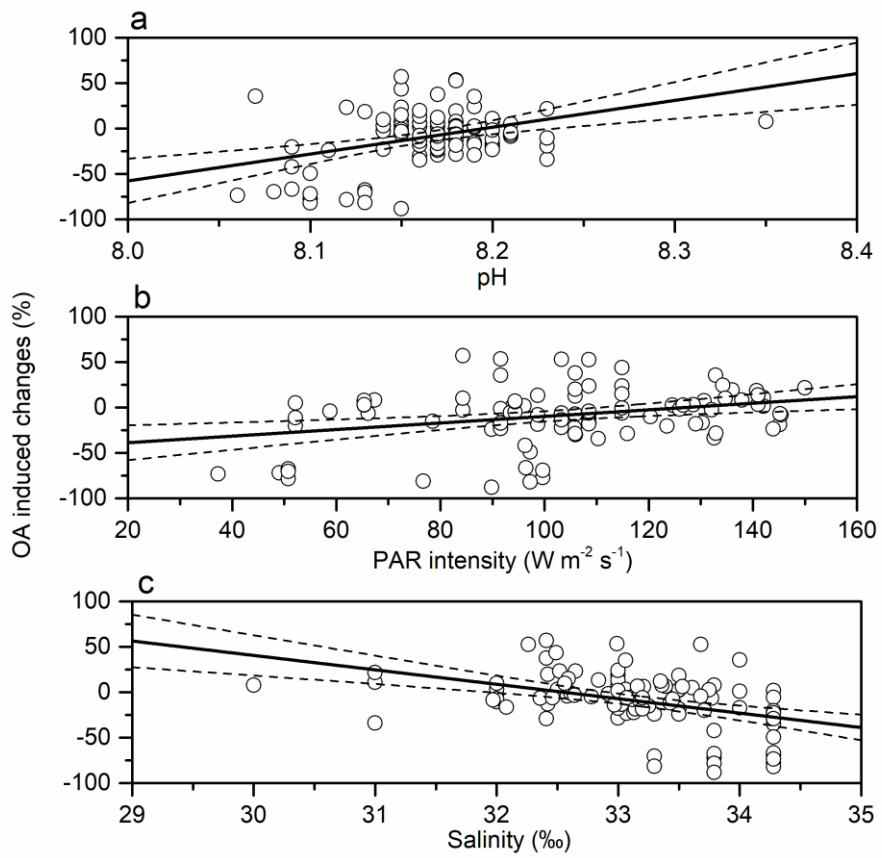
带格式的: 字体: (默认) Times New Roman, 小四, 字体颜色: 文字 1

带格式的: 缩进: 左侧: 0 厘米, 悬挂缩进: 2 字符



带格式的: 字体: (默认) Times New Roman, 小四, 字体颜色: 文字 1

Fig. 5



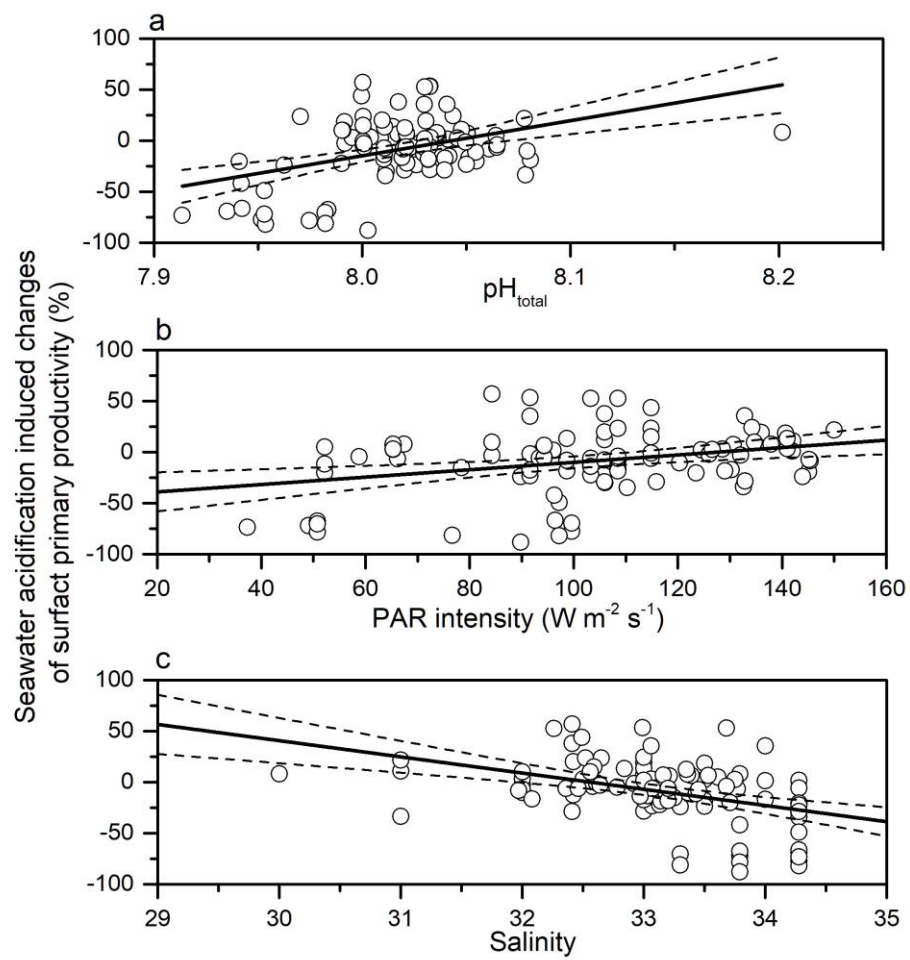


Fig. 6